

Supplementary Information for the exploration and data mining of fungal and oomycetes CAZomes

Emma E. M. Hobbs

June 2023

This document contains all supplementary information for chapter 6 in the thesis Hobbs, 2023. The tables and figures are presented in the same order as they are referenced in the main manuscript.

Contents

1	Genome download	2
2	Exploration of the fungi and oomycetes CAZomes	5
3	Positive selection screening	8
4	<i>In silico</i> characterisation of a PL1 CAZyme AIE	10
4.1	Prediction of a structural fold for PL1 CAZyme AIE	10
4.2	Structural comparison between AIE, PDB:1IDK and PDB:3ZSC	12
5	Positive selection in AIE	14
6	<i>In silico</i> characterisation of a PL3 CAZyme RKL	16

1 Genome download

SI Table 1: Genomic assemblies downloaded from NCBI

Genus	Species	NCBI Taxonomy ID	NCBI Accession Numbers
<i>Aspergillus</i>	<i>fumigatus</i>	NCBI:txid746128	GCA_012656185.1, GCA_012656215.1, GCA_012656165.1, GCA_012656115.1, GCA_012656125.1, GCA_005768625.2, GCA_003069565.1, GCA_002234985.1, GCA_002234955.1, GCA_001715275.2, GCA_001643655.1, GCA_001643665.1
<i>Aspergillus</i>	<i>nidulans</i>	NCBI:txid162425	GCA_011075025.1, GCA_011074995.1
<i>Aspergillus</i>	<i>niger</i>	NCBI:txid5061	GCA_011316255.1, GCA_009812365.1, GCA_004634315.1, GCA_002211485.2, GCA_900248155.1, GCA_002740505.1, GCA_001931795.1, GCA_001741915.1, GCA_001741905.1, GCA_001741885.1, GCA_001715265.1, GCA_001515345.1, GCF_000002855.3
<i>Aspergillus</i>	<i>sydowii</i>	NCBI:txid75750	GCA_009828905.1, GCA_009193685.1
<i>Fusarium</i>	<i>graminearum</i>	NCBI:txid5518	GCA_012959185.1, GCA_006942295.1, GCA_900492705.1, GCA_900476405.1, GCA_002352725.1, GCA_900044135.1, GCA_001717915.1, GCA_001717905.1, GCA_000966635.1, GCA_000966645.1, GCA_000599445.1 GCA_011428085.1, GCA_011426355.1, GCA_011426335.1, GCA_011424645.1, GCA_011424625.1, GCA_011424605.1, GCA_011421335.1, GCA_011421285.1, GCA_011421305.1, GCA_011421375.1, GCA_011421365.1, GCA_011421355.1, GCA_011421275.1, GCA_011421325.1, GCA_011037735.1, GCA_011037105.1, GCA_011037075.1, GCA_011036425.1, GCA_011036365.1, GCA_011036345.1, GCA_011036325.1, GCA_011036305.1, GCA_011036285.1, GCA_011036015.1, GCA_011035995.1, GCA_011035975.1, GCA_011035895.1, GCA_011035875.1, GCA_011035855.1, GCA_011035785.1, GCA_011035765.1, GCA_011035725.1, GCA_011037135.1, GCA_011037005.1, GCA_011036985.1, GCA_011036965.1, GCA_01103695.1, GCA_011036925.1, GCA_011036905.1, GCA_011036835.1, GCA_011035665.1, GCA_011035645.1, GCA_011035625.1, GCA_011035595.1, GCA_011035555.1, GCA_011035525.1, GCA_011036745.1, GCA_011035505.1, GCA_011036685.1, GCA_011036655.1, GCA_011036635.1, GCA_011036615.1, GCA_011035355.1, GCA_011036575.1, GCA_011035205.1, GCA_011035185.1, GCA_011035135.1, GCA_011035015.1, GCA_011034965.1, GCA_011034945.1, GCA_011034875.1, GCA_011034825.1, GCA_011034785.1, GCA_011034745.1, GCA_011034655.1, GCA_011034575.1, GCA_011034545.1, GCA_011034455.1, GCA_011034415.1, GCA_011034375.1, GCA_011034275.1, GCA_011034205.1, GCA_011034135.1, GCA_011034075.1, GCA_011034045.1, GCA_011034025.1, GCA_011037795.1, GCA_011033995.1, GCA_011033925.1, GCA_011033815.1, GCA_011033715.1, GCA_011033745.1, GCA_011033645.1, GCA_011036945.1, GCA_011036875.1, GCA_011036795.1, GCA_011036775.1, GCA_011036815.1, GCA_011036855.1, GCA_011036595.1, GCA_011036705.1, GCA_011036765.1, GCA_011036565.1, GCA_011036545.1, GCA_011036445.1, GCA_011036725.1, GCA_011036505.1, GCA_011036515.1, GCA_011036475.1, GCA_011036455.1, GCA_011036395.1, GCA_011036385.1, GCA_011036275.1, GCA_011036235.1, GCA_011036165.1, GCA_011036225.1, GCA_011036215.1, GCA_011036205.1, GCA_011036075.1, GCA_011036135.1, GCA_011036055.1, GCA_011036065.1, GCA_011036045.1, GCA_011035965.1, GCA_011035955.1, GCA_011035835.1, GCA_011035845.1, GCA_011035825.1, GCA_011035755.1, GCA_011035745.1, GCA_011033685.1, GCA_011033665.1, GCA_011033625.1, GCA_011033575.1, GCA_011033555.1, GCA_011033535.1, GCA_011033505.1, GCA_011033485.1, GCA_011033455.1, GCA_011035615.1, GCA_011035485.1, GCA_011035495.1, GCA_011035455.1, GCA_011035415.1, GCA_011035435.1, GCA_011035375.1, GCA_011035345.1, GCA_011035385.1, GCA_011035335.1, GCA_011035235.1, GCA_011035255.1, GCA_011035245.1, GCA_011035265.1, GCA_011035275.1, GCA_011035075.1, GCA_011035065.1, GCA_011035045.1, GCA_011035055.1, GCA_011035035.1, GCA_011034915.1, GCA_011034925.1, GCA_011034935.1, GCA_011034815.1, GCA_011034845.1, GCA_011034805.1, GCA_011034775.1, GCA_011034735.1, GCA_011034615.1, GCA_011034635.1, GCA_011034645.1, GCA_011034625.1, GCA_011034675.1, GCA_011034565.1, GCA_011034515.1, GCA_011034445.1, GCA_011034485.1, GCA_011034475.1, GCA_011034395.1, GCA_011034265.1, GCA_011034195.1, GCA_011034235.1, GCA_011034155.1, GCA_011034225.1, GCA_011033985.1, GCA_011033945.1, GCA_011034125.1, GCA_011034105.1, GCA_011033955.1, GCA_011033875.1, GCA_011034095.1, GCA_011033805.1, GCA_011033885.1, GCA_011033895.1, GCA_011033765.1, GCA_011033785.1, GCA_011033475.1, GCA_011033595.1, GCA_011033375.1, GCA_011033525.1, GCA_011033385.1, GCA_011032885.1, GCA_011032855.1, GCA_009746015.1, GCA_009299335.1, GCA_009299235.1, GCA_009299215.1, GCA_009299195.1, GCA_009299155.1, GCA_009299095.1, GCA_009299045.1, GCA_009298875.1, GCA_009298855.1, GCA_009298805.1, GCA_009298685.1, GCA_009298645.1, GCA_009298615.1, GCA_009298555.1, GCA_009298505.1, GCA_009298475.1, GCA_009298435.1, GCA_009298405.1, GCA_009298245.1, GCA_009298235.1, GCA_009298205.1, GCA_009298195.1, GCA

2 Exploration of the fungi and oomycetes CAZomes

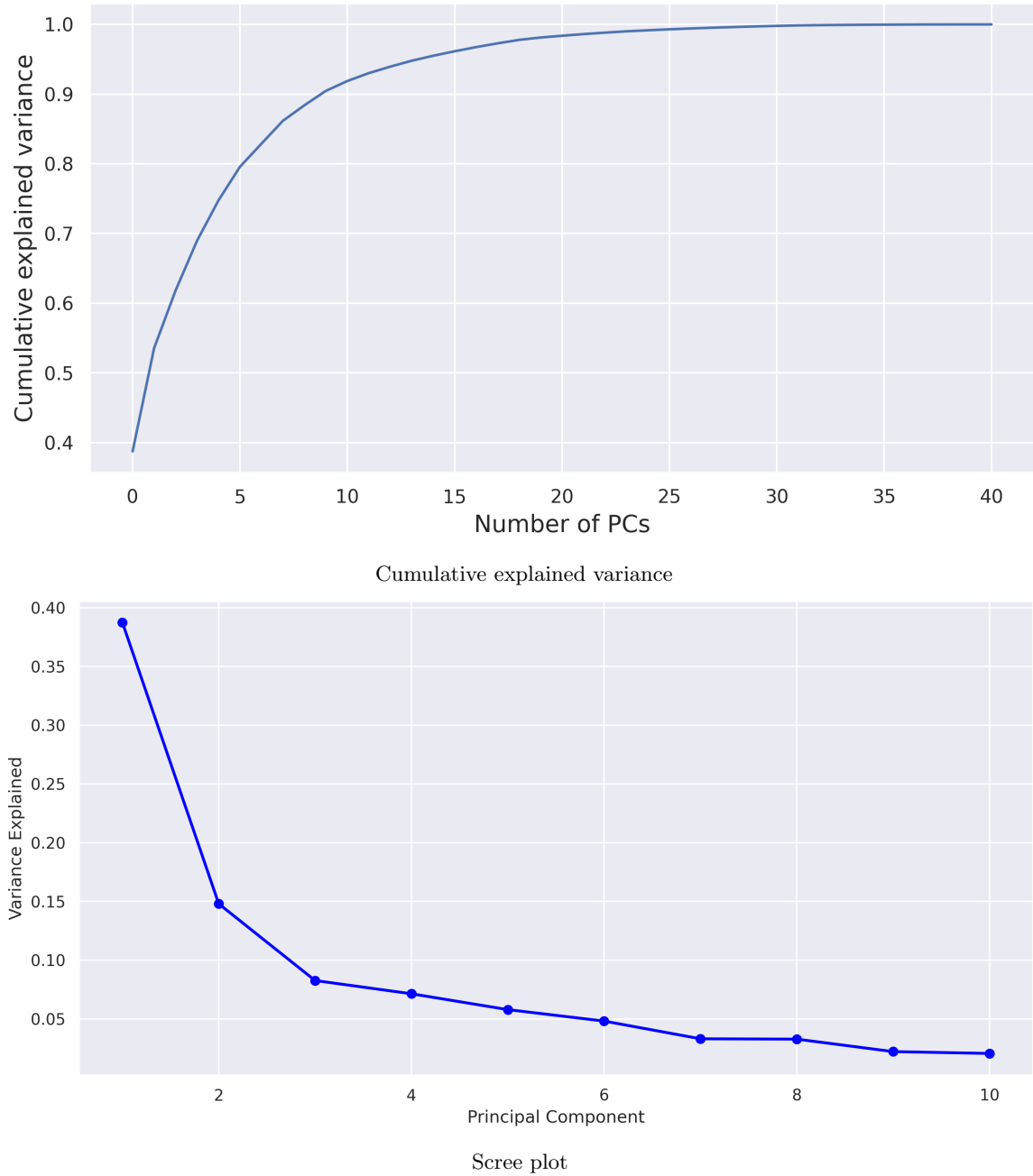
SI Table 2: Output of Tukey HSD test

Group 1	Group 2	Mean Difference	Adjusted P-value	Lower CI	Upper CI	Reject NH
AA-Fungi	AA-Oomycete	-47.066	0.0008	-82.0655	-12.0664	TRUE
AA-Fungi	CBM-Fungi	-12.2188	0.8479	-35.4091	10.9716	FALSE
AA-Fungi	CBM-Oomycete	-49.9549	0.0003	-84.9544	-14.9553	TRUE
AA-Fungi	CE-Fungi	-28.8438	0.0032	-52.0341	-5.6534	TRUE
AA-Fungi	CE-Oomycete	-40.8438	0.0082	-75.8433	-5.8442	TRUE
AA-Fungi	GH-Fungi	211.125	0	187.9347	234.3153	TRUE
AA-Fungi	GH-Oomycete	117.8229	0	82.8233	152.8225	TRUE
AA-Fungi	GT-Fungi	38.1875	0	14.9972	61.3778	TRUE
AA-Fungi	GT-Oomycete	40.2674	0.0099	5.2678	75.2669	TRUE
AA-Fungi	PL-Fungi	-45.8438	0	-69.0341	-22.6534	TRUE
AA-Fungi	PL-Oomycete	-28.9549	0.2178	-63.9544	6.0447	FALSE
AA-Oomycete	CBM-Fungi	34.8472	0.0522	-0.1523	69.8468	FALSE
AA-Oomycete	CBM-Oomycete	-2.8889	1	-46.617	40.8392	FALSE
AA-Oomycete	CE-Fungi	18.2222	0.8579	-16.7773	53.2218	FALSE
AA-Oomycete	CE-Oomycete	6.2222	1	-37.5059	49.9503	FALSE
AA-Oomycete	GH-Fungi	258.191	0	223.1914	293.1905	TRUE
AA-Oomycete	GH-Oomycete	164.8889	0	121.1608	208.617	TRUE
AA-Oomycete	GT-Fungi	85.2535	0	50.2539	120.253	TRUE
AA-Oomycete	GT-Oomycete	87.3333	0	43.6052	131.0615	TRUE
AA-Oomycete	PL-Fungi	1.2222	1	-33.7773	36.2218	FALSE
AA-Oomycete	PL-Oomycete	18.1111	0.9685	-25.617	61.8392	FALSE
CBM-Fungi	CBM-Oomycete	-37.7361	0.0223	-72.7357	-2.7365	TRUE
CBM-Fungi	CE-Fungi	-16.625	0.4329	-39.8153	6.5653	FALSE
CBM-Fungi	CE-Oomycete	-28.625	0.2328	-63.6246	6.3746	FALSE
CBM-Fungi	GH-Fungi	223.3438	0	200.1534	246.5341	TRUE
CBM-Fungi	GH-Oomycete	130.0417	0	95.0421	165.0412	TRUE
CBM-Fungi	GT-Fungi	50.4062	0	27.2159	73.5966	TRUE
CBM-Fungi	GT-Oomycete	52.4861	0.0001	17.4865	87.4857	TRUE
CBM-Fungi	PL-Fungi	-33.625	0.0002	-56.8153	-10.4347	TRUE
CBM-Fungi	PL-Oomycete	-16.7361	0.9152	-51.7357	18.2635	FALSE
CBM-Oomycete	CE-Fungi	21.1111	0.6988	-13.8885	56.1107	FALSE
CBM-Oomycete	CE-Oomycete	9.1111	0.9999	-34.617	52.8392	FALSE
CBM-Oomycete	GH-Fungi	261.0799	0	226.0803	296.0794	TRUE
CBM-Oomycete	GH-Oomycete	167.7778	0	124.0497	211.5059	TRUE
CBM-Oomycete	GT-Fungi	88.1424	0	53.1428	123.1419	TRUE
CBM-Oomycete	GT-Oomycete	90.2222	0	46.4941	133.9503	TRUE
CBM-Oomycete	PL-Fungi	4.1111	1	-30.8885	39.1107	FALSE
CBM-Oomycete	PL-Oomycete	21	0.9128	-22.7281	64.7281	FALSE
CE-Fungi	CE-Oomycete	-12	0.9929	-46.9996	22.9996	FALSE
CE-Fungi	GH-Fungi	239.9688	0	216.7784	263.1591	TRUE
CE-Fungi	GH-Oomycete	146.6667	0	111.6671	181.6662	TRUE
CE-Fungi	GT-Fungi	67.0312	0	43.8409	90.2216	TRUE
CE-Fungi	GT-Oomycete	69.1111	0	34.1115	104.1107	TRUE
CE-Fungi	PL-Fungi	-17	0.3967	-40.1903	6.1903	FALSE
CE-Fungi	PL-Oomycete	-0.1111	1	-35.1107	34.8885	FALSE
CE-Oomycete	GH-Fungi	251.9688	0	216.9692	286.9683	TRUE
CE-Oomycete	GH-Oomycete	158.6667	0	114.9385	202.3948	TRUE
CE-Oomycete	GT-Fungi	79.0312	0	44.0317	114.0308	TRUE
CE-Oomycete	GT-Oomycete	81.1111	0	37.383	124.8392	TRUE
CE-Oomycete	PL-Fungi	-5	1	-39.9996	29.9996	FALSE
CE-Oomycete	PL-Oomycete	11.8889	0.9991	-31.8392	55.617	FALSE
GH-Fungi	GH-Oomycete	-93.3021	0	-128.3017	-58.3025	TRUE
GH-Fungi	GT-Fungi	-172.9375	0	-196.1278	-149.7472	TRUE
GH-Fungi	GT-Oomycete	-170.8576	0	-205.8572	-135.8581	TRUE
GH-Fungi	PL-Fungi	-256.9688	0	-280.1591	-233.7784	TRUE
GH-Fungi	PL-Oomycete	-240.0799	0	-275.0794	-205.0803	TRUE
GH-Oomycete	GT-Fungi	-79.6354	0	-114.635	-44.6358	TRUE
GH-Oomycete	GT-Oomycete	-77.5556	0	-121.2837	-33.8274	TRUE
GH-Oomycete	PL-Fungi	-163.6667	0	-198.6662	-128.6671	TRUE
GH-Oomycete	PL-Oomycete	-146.7778	0	-190.5059	-103.0497	TRUE
GT-Fungi	GT-Oomycete	2.0799	1	-32.9197	37.0794	FALSE
GT-Fungi	PL-Fungi	-84.0312	0	-107.2216	-60.8409	TRUE
GT-Fungi	PL-Oomycete	-67.1424	0	-102.1419	-32.1428	TRUE
GT-Oomycete	PL-Fungi	-86.1111	0	-121.1107	-51.1115	TRUE
GT-Oomycete	PL-Oomycete	-69.2222	0	-112.9503	-25.4941	TRUE
PL-Fungi	PL-Oomycete	16.8889	0.9101	-18.1107	51.8885	FALSE

Output from a post hoc TukeyHSD test following a two-way ANOVA testing for statistically significant differences between CAZy class frequencies between fungi and oomycetes.

SI Figure 1: Cumulative explained frequency and scree plot of principal component analysis of CAZyme family frequencies in fungi and oomycetes

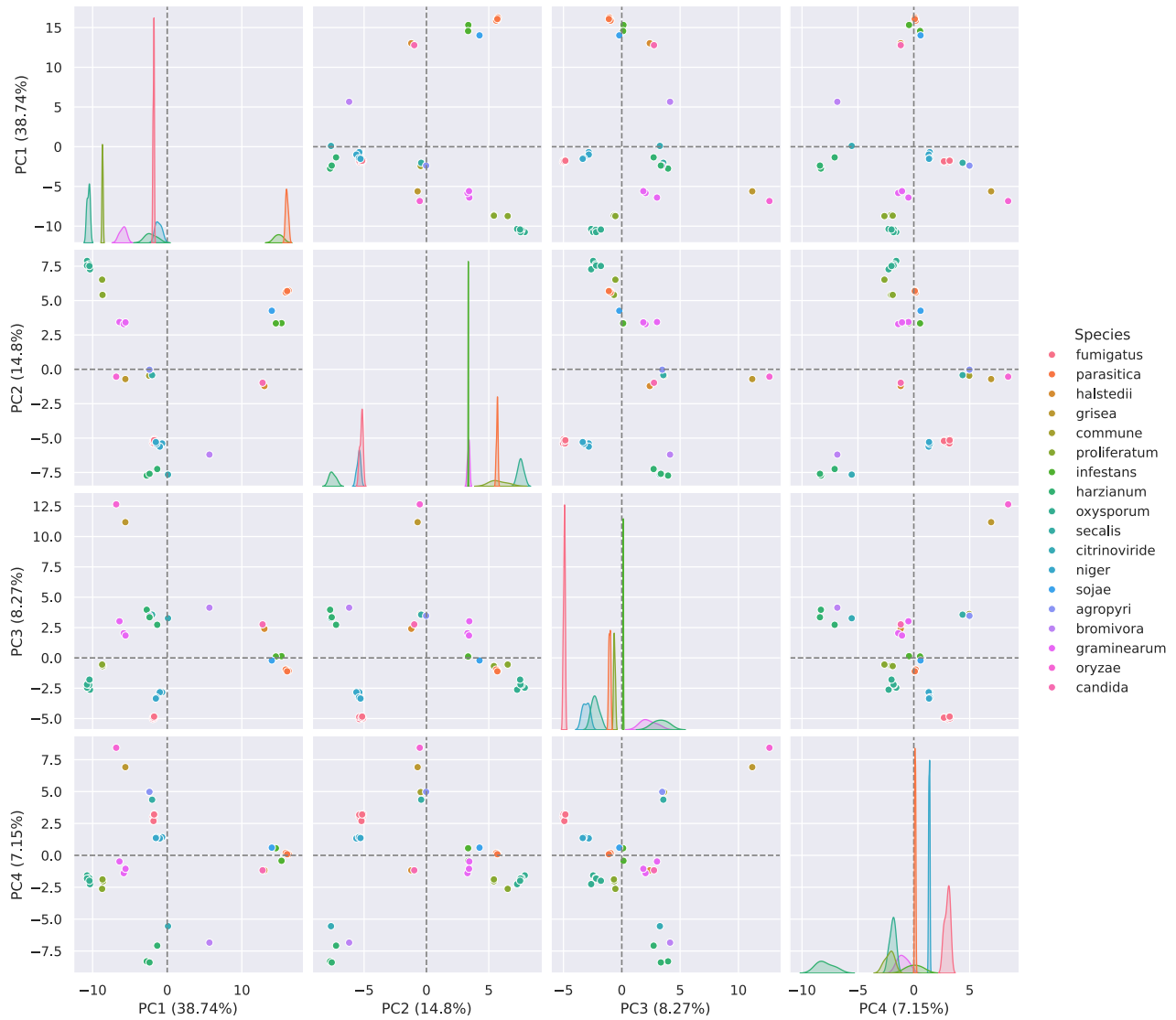
CAZyme family frequencies are the number of unique protein IDs assigned to each CAZyme family.



Principal component analysis (PCA) of the CAZy family frequencies in *Pectobacteriaceae* genomes, plotting [A] the cumulative frequency across all computed principal components (PCs). [B] Scree plot plotting the fraction of variance captured by each PC.

SI Figure 2: Principal component analysis of fungal and oomycete CAZyme family frequencies, with genomes colour coded by species

CAZyme family frequencies are the number of unique protein IDs assigned to each CAZyme family.



Principal component analysis of CAZy family frequencies in fungi and oomycete

Genomes are projected onto all combinations of principal components (PCs) PC1-PC4. KDE plots (univariate distribution plots) are plotted on the diagonal, showing the marginal distribution of genomes in each column, colour-coded by species classifications. Scatter plots are colour-coded and styled by species classification.

3 Positive selection screening

SI Table 3: Output from aBSREL for cluster AAA32701

Output from aBSREL for cluster AAA32701. Rows highlighted in green indicate the detection of positive selection

Name	B	LRT	Test p-value	Uncorrected p-value	ω distribution over sites
AAM23009_1	0.172	74.271	0	0	$\omega_1 = 0.00$ (81%) $\omega_2 = 117$ (19%)
AIE38009_1	0.017	27.042	0	0	$\omega_1 = 0.0257$ (99%) $\omega_2 = \infty$ (1.3%)
Node29	0.103	17.924	0.001	0	$\omega_1 = 0.320$ (93%) $\omega_2 = 36.3$ (7.0%)
CAP80630_1	0.043	15.839	0.004	0.0001	$\omega_1 = 0.0483$ (96%) $\omega_2 = 5000$ (4.1%)
BAB82468_1	0.003	6.4616	0.408	0.0141	$\omega_1 = 0.0805$ (100%) $\omega_2 = 1500$ (0.37%)
Node6	0.062	5.623	0.604	0.0216	$\omega_1 = 0.144$ (95%) $\omega_2 = 519$ (4.8%)
Node16	0.068	5.4419	0.639	0.0237	$\omega_1 = 0.0754$ (97%) $\omega_2 = 5000$ (3.1%)
AAA32701_1	0	0	1	1	$\omega_1 = 1.00$ (100%)
AFS18475_1	0	0	1	1	$\omega_1 = 1.00$ (100%)
AGV28619_1	0	0	1	1	$\omega_1 = 1.00$ (100%)
BAE65949_1	0	0	1	1	$\omega_1 = 1.00$ (100%)
BCR99717_1	0	0	1	1	$\omega_1 = 1.00$ (100%)
CAK47350_1	0	0	1	1	$\omega_1 = 1.00$ (100%)
GAA92866_1	0	0	1	1	$\omega_1 = 1.00$ (100%)
GAQ43951_1	0.008	0	1	1	$\omega_1 = 0.0295$ (100%)
Node1	0.013	0	1	1	$\omega_1 = 0.0292$ (100%)
Node12	1E-04	0	1	1	$\omega_1 = 1.00$ (100%)
Node17	0.01	0	1	1	$\omega_1 = 0.0664$ (100%)
Node19	0.003	0	1	1	$\omega_1 = 0.156$ (100%)
Node22	0.013	3.5707	1	0.0621	$\omega_1 = 0.000773$ (97%) $\omega_2 = 13.1$ (3.2%)
Node23	0.002	0	1	1	$\omega_1 = 0.950$ (100%)
Node24	0	0	1	1	$\omega_1 = 0.00$ (100%)
Node31	0	0	1	1	$\omega_1 = 1.00$ (100%)
Node4	0.05	0.4531	1	0.3394	$\omega_1 = 0.00$ (92%) $\omega_2 = 2.10$ (7.6%)
Node5	0.094	3.777	1	0.0558	$\omega_1 = 0.0448$ (92%) $\omega_2 = \infty$ (7.6%)
Node7	0.002	0	1	1	$\omega_1 = 0.00$ (100%)
Node8	0	0	1	1	$\omega_1 = 1.00$ (100%)
OXN15357_1	0.171	0	1	1	$\omega_1 = 0.00129$ (85%) $\omega_2 = 0.517$ (15%)
QMW36737_1	0	0	1	1	$\omega_1 = 1.00$ (100%)
QMW48793_1	0	0	1	1	$\omega_1 = 1.00$ (100%)
QQK48079_1	0	0	1	1	$\omega_1 = 1.00$ (100%)
QRD92196_1	0	0	1	1	$\omega_1 = 1.00$ (100%)
SPB48655_1	0	0	1	1	$\omega_1 = 1.00$ (100%)

SI Table 4: Output from aBSREL for RKK95495 cluster

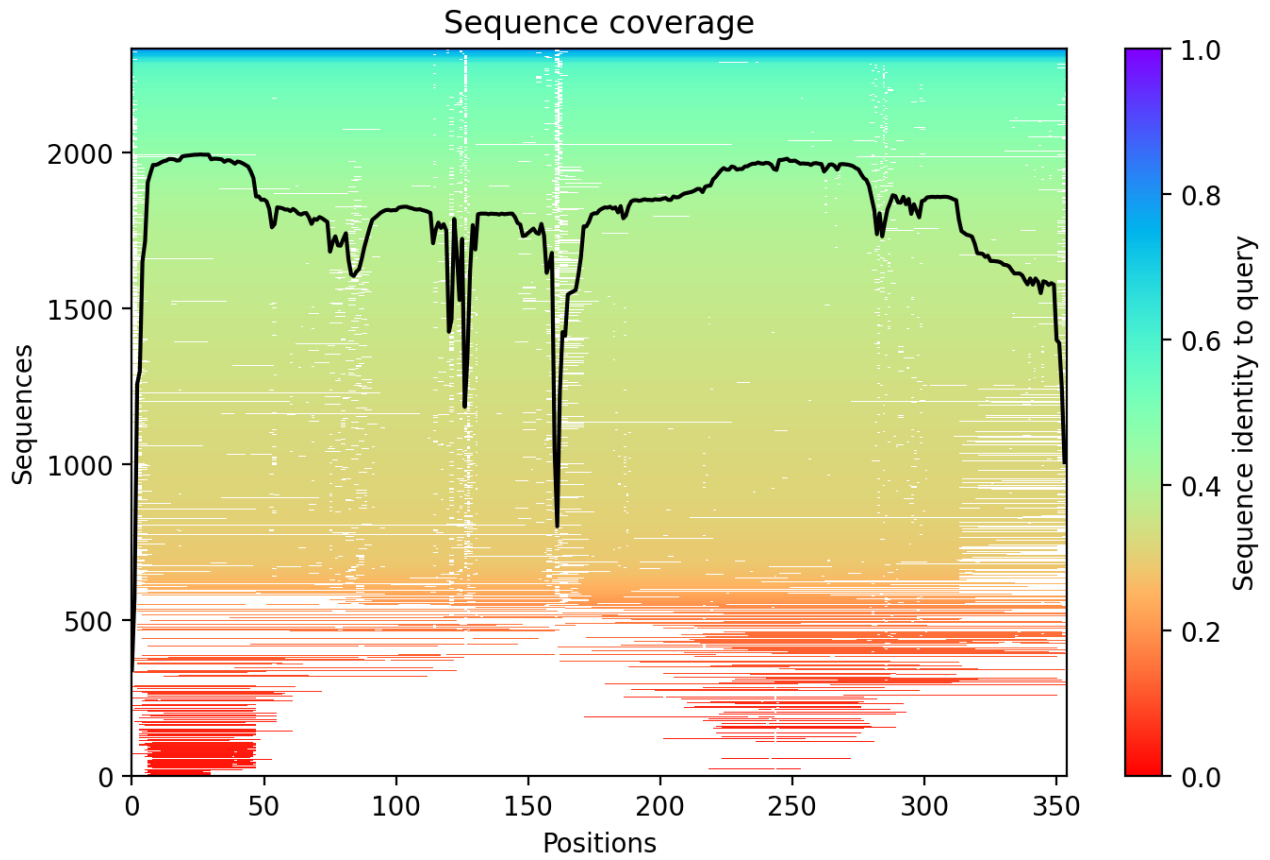
Output from aBSREL for cluster RKK95495. Rows highlighted in green indicate the detection of positive selection

Name	B	LRT	Test p-value	Uncorrected p-value	ω distribution over sites
RKL00490.1	0.0278	30.2322	0	0	$\omega_1 = 0.274$ (98%) $\omega_2 = \infty$ (2.3%)
AAC49420.1	0.1071	10.6468	0.0943	0.0017	$\omega_1 = 0.0594$ (95%) $\omega_2 = 26.0$ (4.6%)
Node41	0.0419	7.6034	0.4326	0.0079	$\omega_1 = 0.656$ (99%) $\omega_2 = \infty$ (0.72%)
CEI68085.1	0.0427	6.4403	0.7677	0.0142	$\omega_1 = 0.0399$ (99%) $\omega_2 = \infty$ (1.2%)
CCT64935.1	0	0	1	1	$\omega_1 = 1.00$ (100%)
CEF86969.1	0.0014	-27.7065	1	0.5	$\omega_1 = 10000000000$ (100%)
CEF87884.1	0	0	1	1	$\omega_1 = 1.00$ (100%)
CEI70384.1	0.0179	0	1	1	$\omega_1 = 0.0134$ (100%)
CZS83373.1	0	0	1	1	$\omega_1 = 1.00$ (100%)
CZS85704.1	0	0	1	1	$\omega_1 = 1.00$ (100%)
Node1	0	0	1	1	$\omega_1 = 1.00$ (100%)
Node10	0.0665	0	1	1	$\omega_1 = 0.133$ (100%)
Node12	0.007	0	1	1	$\omega_1 = 0.00$ (100%)
Node13	0.016	0	1	1	$\omega_1 = 0.00$ (100%)
Node17	0.0813	1.0815	1	0.2344	$\omega_1 = 0.00$ (97%) $\omega_2 = 3.31$ (2.9%)
Node18	0.0464	0	1	1	$\omega_1 = 0.0167$ (100%)
Node20	0.0287	0	1	1	$\omega_1 = 0.0271$ (100%)
Node21	0.021	0	1	1	$\omega_1 = 0.00$ (100%)
Node22	0	-27.662	1	0.5	$\omega_1 = 10000000000$ (100%)
Node23	0	0	1	1	$\omega_1 = 1.00$ (100%)
Node29	0.0955	0	1	1	$\omega_1 = 0.00362$ (100%)
Node30	0.001	0	1	1	$\omega_1 = 0.00$ (100%)
Node31	0	0	1	1	$\omega_1 = 1.00$ (100%)
Node32	0	0	1	1	$\omega_1 = 1.00$ (100%)
Node37	0.0096	0.0264	1	0.4703	$\omega_1 = 10000000000$ (100%)
Node4	0.0155	0	1	1	$\omega_1 = 0.00$ (100%)
Node43	0.0395	4.1898	1	0.0451	$\omega_1 = 0.00$ (99%) $\omega_2 = 17.3$ (0.93%)
Node45	0.0057	0	1	1	$\omega_1 = 0.0819$ (100%)
Node46	0.0189	0	1	1	$\omega_1 = 0.0535$ (100%)
Node47	0.0014	0.6034	1	0.3093	$\omega_1 = 10000000000$ (100%)
Node5	0.0569	0	1	1	$\omega_1 = 0.0304$ (100%)
Node52	0.0214	0	1	1	$\omega_1 = 0.0128$ (100%)
Node55	0.0016	0	1	1	$\omega_1 = 0.00$ (100%)
Node6	0.0544	2.5251	1	0.1073	$\omega_1 = 0.00$ (97%) $\omega_2 = 65.9$ (2.9%)
Node7	0.1663	0	1	1	$\omega_1 = 0.00156$ (94%) $\omega_2 = 0.108$ (5.6%)
Node8	0.1017	4.2612	1	0.0434	$\omega_1 = 0.00$ (93%) $\omega_2 = 23.9$ (6.6%)
PCD34109.1	0.0377	0.4506	1	0.3399	$\omega_1 = 0.00$ (95%) $\omega_2 = 2.14$ (5.1%)
PCD36610.1	0	0	1	1	$\omega_1 = 1.00$ (100%)
QGI61249.1	0	0	1	1	$\omega_1 = 1.00$ (100%)
QGI78430.1	0	-28.6058	1	0.5	$\omega_1 = 10000000000$ (100%)
QGI92147.1	0	0	1	1	$\omega_1 = 1.00$ (100%)
QKD53642.1	0	0	1	1	$\omega_1 = 0.00$ (100%)
QKD61417.1	0	0	1	1	$\omega_1 = 1.00$ (100%)
QPC62756.1	0.0145	0	1	1	$\omega_1 = 0.0723$ (100%)
QPC78206.1	0.0331	0	1	1	$\omega_1 = 0.0135$ (100%)
QPC80127.1	0.0153	0	1	1	$\omega_1 = 0.0646$ (100%)
RBA14607.1	0	0.5816	1	0.3134	$\omega_1 = 10000000000$ (100%)
RBA19176.1	0.0196	0	1	1	$\omega_1 = 0.171$ (100%)
RKK70046.1	0.0026	0	1	1	$\omega_1 = 0.171$ (100%)
RKK75521.1	0.0088	0	1	1	$\omega_1 = 0.0696$ (100%)
RKK88712.1	0	0	1	1	$\omega_1 = 0.00$ (100%)
RKK95495.1	0.0015	0	1	1	$\omega_1 = 0.169$ (100%)
RKK99321.1	0	-27.6767	1	0.5	$\omega_1 = 10000000000$ (100%)
RKL26876.1	0	0	1	1	$\omega_1 = 1.00$ (100%)
RKL28993.1	0.0278	0	1	1	$\omega_1 = 0.00$ (100%)
RKL50686.1	0.0027	0.5786	1	0.314	$\omega_1 = 10000000000$ (100%)
SCO85995.1	0.0042	0	1	1	$\omega_1 = 0.365$ (100%)

4 *In silico* characterisation of a PL1 CAZyme AIE

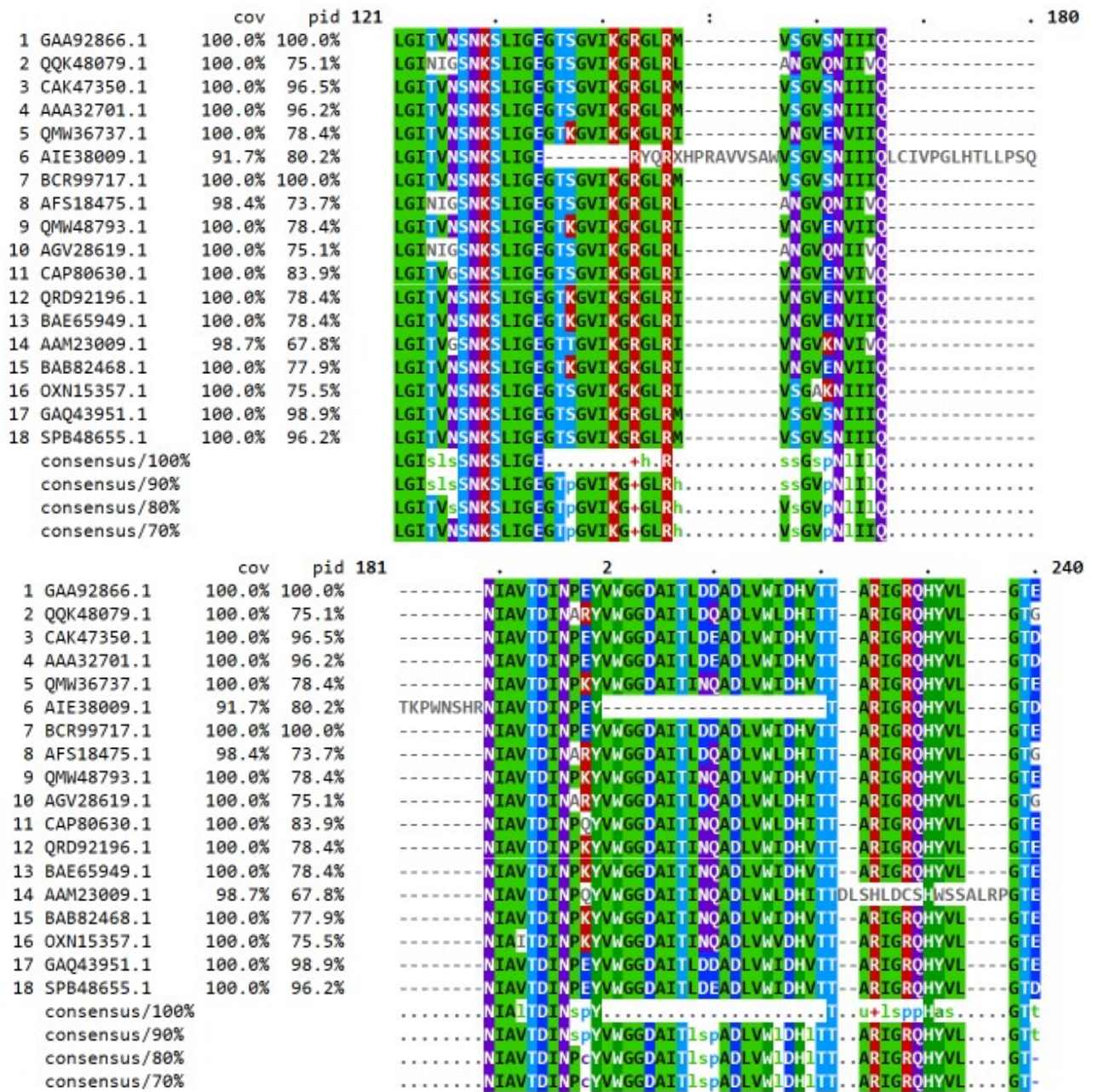
4.1 Prediction of a structural fold for PL1 CAZyme AIE

SI Figure 3: Sequence coverage by ColabFold



Sequence coverage of protein sequence of NCBI:AIE38009.1 by an MSA generated by ColabFold

SI Figure 4: Multi-sequence alignment of AAA32701 cluster members



Multi-sequence alignment of AAA32701 cluster members

4.2 Structural comparison between AIE, PDB:1IDK and PDB:3ZSC

SI Table 5: Output from Dali server, screening for structural homologs to AIE against the RCSB PDB database (October 2022)

Table 1: Output from Dali server, screening for structural homologs to AIE against the RCSB PDB database (October 2022)

PDB (Chain)	DALI Z- Score	RMSD (Å)	lali	nres	% Iden- tity	Function	Organism	Citation
1idk-(A)	44.3	1.7	170	338	59	Pectin Lyase	Aspergillus niger	Mayans et al., 1997
3zsc-(A)	28.6	2.3	259	329	22	Pectate Lyase	Thermotoga maritima	McDonough et al., 2020
2qy1-(A)	27.6	2.6	257	330	20	Pectate Lyase	Xanthomonas campestris	Xiao et al., 2008

SI Figure 5: Sequence alignment between AIE, PDB:1IDK and PDB:3ZSC

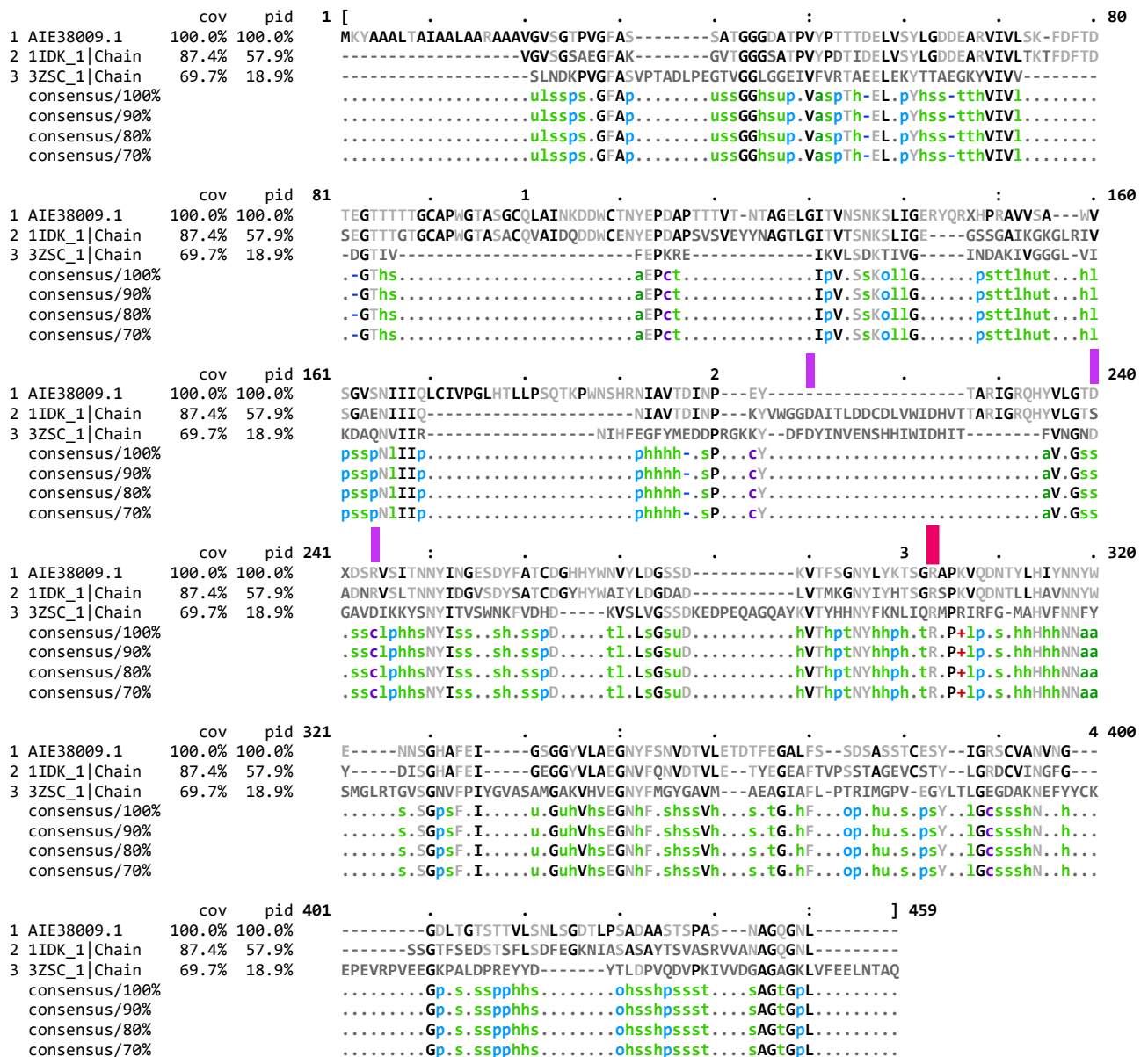


Figure 2: Protein sequence alignment of AIE, PDB:1IDK and PDB:3ZSC, visualised using MView (at <https://www.ebi.ac.uk/Tools/msa/mview/>)

5 Positive selection in AIE

SI Table 6: Output from CodeML, detecting sites of positive selection within AIE

Table 2: Output from CodeML Branch site model: Bayes Empirical Bayes (BEB) analysis to detect positive sites for foreground lineages Prob(w_i1) (*P_i0.95, **P_i0.99)

Position	Residue	P-value	Position	Residue	P-value	Position	Residue	P-value
67	F	1.000**	113	T	0.999**	155	Q	1.000**
68	D	0.999**	114	N	0.952*	156	L	1.000**
69	F	0.999**	115	T	1.000**	157	C	0.999**
70	T	1.000**	116	A	0.998**	159	V	0.973*
71	D	0.999**	117	G	0.999**	160	P	1.000**
72	T	0.999**	118	E	0.999**	161	G	1.000**
73	E	1.000**	119	L	1.000**	162	L	1.000**
74	G	0.999**	120	G	0.985*	163	H	1.000**
75	T	0.999**	121	I	0.961*	164	T	0.975*
80	G	0.998**	122	T	0.999**	165	L	1.000**
81	C	0.965*	123	V	0.946	166	L	0.999**
82	A	1.000**	124	N	0.952*	167	P	1.000**
83	P	0.886	125	S	0.999**	168	S	1.000**
84	W	1.000**	127	K	1.000**	169	Q	1.000**
85	G	0.995**	128	S	0.999**	170	T	1.000**
86	T	1.000**	129	L	1.000**	171	K	1.000**
87	A	0.959*	130	I	0.999**	172	P	1.000**
88	S	0.953*	131	G	1.000**	173	W	1.000**
89	G	0.999**	132	E	1.000**	174	N	0.970*
90	C	0.83	133	R	0.997**	175	S	0.958*
91	Q	1.000**	134	Y	0.999**	176	H	0.958*
92	L	0.979*	135	Q	1.000**	177	R	1.000**
93	A	0.999**	136	R	1.000**	178	N	0.995**
94	I	0.999**	137	H	1.000**	179	I	1.000**
95	N	0.954*	138	P	1.000**	180	A	0.964*
96	K	0.956*	139	R	0.999**	181	V	0.998**
97	D	0.999**	140	A	1.000**	182	T	0.999**
99	W	1.000**	141	V	0.977*	183	D	1.000**
100	C	0.968*	142	V	0.997**	185	N	0.943
101	T	1.000**	143	S	1.000**	186	P	0.956*
102	N	0.95	144	A	1.000**	187	E	0.998**
103	Y	0.957*	145	W	0.999**	188	Y	1.000**
104	E	0.999**	146	V	0.997**	216	F	0.964*
105	P	1.000**	147	S	0.999**			
106	D	1.000**	148	G	0.960*			
107	A	0.931	149	V	0.968*			
108	P	0.964*	150	S	0.999**			
109	T	0.959*	151	N	0.980*			
112	V	0.995**	152	I	0.954*			

SI Table 7: Output of MEME, detecting positive selection in AIE

Table 3: Sites of positive selection in the protein sequences of cluster AAA32701, detected by MEME

Codon	Partition	alpha	beta+	p+	LRT	Episodic selection detected?	branches	Significance
28	1	0.379	1186.8	0.06	13.1	Yes, p = 0.0006	1	**
32	1	0	7.4	0.21	6	Yes, p = 0.0225	2	*
126	1	0	6.5	0.1	4.5	Yes, p = 0.0494	1	*
144	1	0.366	1889.3	0.06	14.1	Yes, p = 0.0004	1	**
305	1	0	37.3	0.15	7.6	Yes, p = 0.0098	0	**
414	1	0	10.6	0.19	5.2	Yes, p = 0.0340	2	*

6 *In silico* characterisation of a PL3 CAZyme RKL

SI Table 8: Output from CodeML, detecting sites of positive selection within RKL

Table 4: Output from CodeML Branch site model: Bayes Empirical Bayes (BEB) analysis to detect positive sites for foreground lineages Prob(w>1) (*P_i0.95, **P_i0.99)

Position	Residue	P-value	Position	Residue	P-value	Position	Residue	P-value
67	F	1.000**	113	T	0.999**	155	Q	1.000**
68	D	0.999**	114	N	0.952*	156	L	1.000**
69	F	0.999**	115	T	1.000**	157	C	0.999**
70	T	1.000**	116	A	0.998**	159	V	0.973*
71	D	0.999**	117	G	0.999**	160	P	1.000**
72	T	0.999**	118	E	0.999**	161	G	1.000**
73	E	1.000**	119	L	1.000**	162	L	1.000**
74	G	0.999**	120	G	0.985*	163	H	1.000**
75	T	0.999**	121	I	0.961*	164	T	0.975*
80	G	0.998**	122	T	0.999**	165	L	1.000**
81	C	0.965*	123	V	0.946	166	L	0.999**
82	A	1.000**	124	N	0.952*	167	P	1.000**
83	P	0.886	125	S	0.999**	168	S	1.000**
84	W	1.000**	127	K	1.000**	169	Q	1.000**
85	G	0.995**	128	S	0.999**	170	T	1.000**
86	T	1.000**	129	L	1.000**	171	K	1.000**
87	A	0.959*	130	I	0.999**	172	P	1.000**
88	S	0.953*	131	G	1.000**	173	W	1.000**
89	G	0.999**	132	E	1.000**	174	N	0.970*
90	C	0.83	133	R	0.997**	175	S	0.958*
91	Q	1.000**	134	Y	0.999**	176	H	0.958*
92	L	0.979*	135	Q	1.000**	177	R	1.000**
93	A	0.999**	136	R	1.000**	178	N	0.995**
94	I	0.999**	137	H	1.000**	179	I	1.000**
95	N	0.954*	138	P	1.000**	180	A	0.964*
96	K	0.956*	139	R	0.999**	181	V	0.998**
97	D	0.999**	140	A	1.000**	182	T	0.999**
99	W	1.000**	141	V	0.977*	183	D	1.000**
100	C	0.968*	142	V	0.997**	185	N	0.943
101	T	1.000**	143	S	1.000**	186	P	0.956*
102	N	0.95	144	A	1.000**	187	E	0.998**
103	Y	0.957*	145	W	0.999**	188	Y	1.000**
104	E	0.999**	146	V	0.997**	216	F	0.964*
105	P	1.000**	147	S	0.999**			
106	D	1.000**	148	G	0.960*			
107	A	0.931	149	V	0.968*			
108	P	0.964*	150	S	0.999**			
109	T	0.959*	151	N	0.980*			
112	V	0.995**	152	I	0.954*			

SI Table 9: Output of MEME, detecting positive selection in RKL

Table 5: Sites of positive selection in the protein sequences of cluster RKK95495, detected by MEME

Codon	Partition	alpha	beta+	p+	LRT	Episodic selection detected?	branches	Significance
192	1	0	0	0.4	6.98	Yes, p = 0.01	2	**
197	1	0	0	0.09	5.7	Yes, p = 0.03	1	*

SI table 10: Prediction of N-glycosylation in RKL

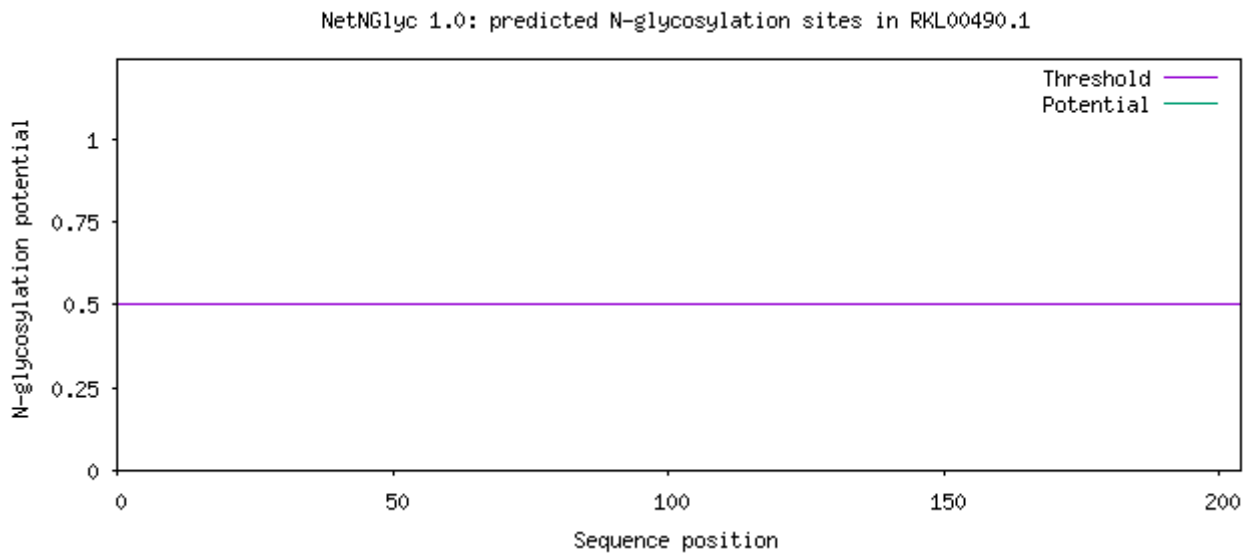


Figure 3: Output from NetNGlyc, predicting sites of N-glycosylation in RKL00490.1

SI table 11: Prediction of O-glycosylation in RKL

Table 6: Output from NetOGlyc, predicting sites of O-glycosylation in RKL00490.1

Sequence name	Start	End	Score	Strand	Frame	Comment
RKL00490.1	5	5	0.370576	.	.	
RKL00490.1	11	11	0.104116	.	.	
RKL00490.1	15	15	0.28624	.	.	
RKL00490.1	23	23	0.645302	.	.	POSITIVE
RKL00490.1	30	30	0.662159	.	.	POSITIVE
RKL00490.1	32	32	0.52429	.	.	POSITIVE
RKL00490.1	34	34	0.683784	.	.	POSITIVE
RKL00490.1	36	36	0.612201	.	.	POSITIVE
RKL00490.1	46	46	0.29102	.	.	
RKL00490.1	61	61	0.203508	.	.	
RKL00490.1	62	62	0.384798	.	.	
RKL00490.1	71	71	0.067379	.	.	
RKL00490.1	99	99	1.76E-05	.	.	
RKL00490.1	101	101	0.003115	.	.	
RKL00490.1	116	116	0.01325	.	.	
RKL00490.1	122	122	0.066702	.	.	
RKL00490.1	162	162	0.022455	.	.	
RKL00490.1	173	173	0.059815	.	.	
RKL00490.1	179	179	0.105596	.	.	
RKL00490.1	180	180	0.213795	.	.	
RKL00490.1	192	192	0.004492	.	.	